

Germline *MYOF1::WNK4* and *VPS25::MYOF1* Chimeras Generated by the Constitutional Translocation *t(17;19)(q21;p13)* in Two Siblings With Myelodysplastic Syndrome

IOANNIS PANAGOPOULOS¹, KRISTIN ANDERSEN¹, VIDAR STAVSETH²,
SYNNE TORKILDSEN³, SVERRE HEIM^{1,4} and MAREN RANDI TANDSÆTHER¹

¹Section for Cancer Cytogenetics, Institute for Cancer Genetics and Informatics,
The Norwegian Radium Hospital, Oslo University Hospital, Oslo, Norway;

²Department of Haematology, Levanger Hospital, Levanger, Norway;

³Department of Haematology, Oslo University Hospital Rikshospitalet, Oslo, Norway;

⁴Institute for Clinical Medicine, Faculty of Medicine, University of Oslo, Oslo, Norway

Abstract. *Background/Aim:* Constitutional chromosomal aberrations are rare in hematologic malignancies and their pathogenetic role is mostly poorly understood. We present a comprehensive molecular characterization of a novel constitutional chromosomal translocation found in two siblings – sisters – diagnosed with myelodysplastic syndrome (MDS). *Materials and Methods:* Bone marrow and blood cells from the two patients were examined using G-banding, RNA sequencing, PCR, and Sanger sequencing. *Results:* We identified a balanced *t(17;19)(q21;p13)* translocation in both siblings' bone marrow, blood cells, and phytohemagglutinin-stimulated lymphocytes. The translocation generated a *MYO1F::WNK4* chimera on the *der(19)t(17;19)*, encoding a chimeric serine/threonine kinase, and a *VPS25::MYO1F* on the *der(17)*, potentially resulting in an aberrant *VPS25* protein. *Conclusion:* The *t(17;19)(q21;p13)* translocation found in the two sisters probably predisposed them to myelodysplasia. How the *MYO1F::WNK4* and/or *VPS25::MYO1F* chimeras, perhaps especially *MYO1F::WNK4* that encodes a chimeric

serine/threonine kinase, played a role in MDS pathogenesis, remains incompletely understood.

Acquired chromosome abnormalities, not least balanced translocations, are key pathogenetic elements in leukemogenesis as extensively reviewed over the last few decades (1-3). These aberrations often give rise to fusion genes that play a pivotal role in the pathogenesis of these neoplasms. A fusion gene, defined as the physical juxtaposition of distinct gene loci, results in a chimeric structure combining one gene's head with the other one's tail (4, 5). Fusion genes are often primary neoplasia-inducing events whose detection is important for the diagnosis, prognosis assessment, and treatment of cancer patients (3, 6, 7).

Constitutional chromosomal aberrations are present in all cells. They occur *de novo* in the gametes or are inherited from a carrier parent. Occasionally, constitutional aberrations are found also in solid cancer families and molecular investigations of such family members have led to the identification of several tumor suppressor genes (8, 9). Much less frequently, constitutional chromosomal rearrangements have also been reported in patients suffering from hematologic malignancies, although their leukemogenic role is mostly unclear (8-20). In this study, we present a detailed molecular characterization of a novel constitutional chromosomal translocation identified in two siblings diagnosed with myelodysplastic syndrome (MDS).

Correspondence to: Ioannis Panagopoulos, Section for Cancer Cytogenetics, Institute for Cancer Genetics and Informatics, The Norwegian Radium Hospital, Oslo University Hospital, P.O. Box 4953 Nydalen, NO-0424 Oslo, Norway. Tel: +47 22934424, email: ioapan@ous-hf.no

Key Words: Myelodysplastic syndrome (MDS), constitutional chromosomal translocation, *t(17;19)(q21;p13)*, *MYO1F*, *WNK4*, *MYO1F::WNK4*, *VPS25::MYO1F*.

Materials and Methods

Ethics statement. The study was approved by the regional ethics committee (Regional komité for medisinsk forskningsetikk Sør-Øst, Norge, <http://helseforskning.etikkom.no>). The administrator of the approval application is the leader of the Section for Cancer Cytogenetics Francesca Micci (Regional komité for medisinsk



This article is an open access article distributed under the terms and conditions of the Creative Commons Attribution (CC BY-NC-ND) 4.0 international license (<https://creativecommons.org/licenses/by-nc-nd/4.0>).

forskningsetikk Sør-Øst, Norge, [http://helseforskning.etikkom.no;2010/1389/REK sør-øst A](http://helseforskning.etikkom.no;2010/1389/REK_sør-øst_A)). Written informed consent was obtained from the patients. The ethics committee's approval included a review of the consent procedure. All patient information has been de-identified.

Patients.

Patient 1. A 63-year-old woman was initially referred to a hematologist in 2013 for mild thrombocytopenia. Due to a previous transient ischemic attack (TIA), she was undergoing aspirin (ASA) treatment. Her hemoglobin (Hgb) was within the normal range, but the mean corpuscular volume (MCV) was slightly elevated at 103 fl. The neutrophil count was also normal at $2.2 \times 10^9/l$. In light of this, no further investigations were pursued at that time. In 2015, she was re-referred due to pancytopenia with an Hgb of 11.5 g/dl and an MCV of 109. Neutrophils had decreased to $0.9 \times 10^9/l$ and platelet count was at $54 \times 10^9/l$. A bone marrow smear indicated low cellularity with a normal blast count of 1%. No ringed sideroblasts were observed. A subsequent bone marrow biopsy revealed hypoplastic and dysplastic changes. G-banding identified a t(17;19)(q21;p13) translocation in all 3 metaphases analyzed (see cytogenetic examination below). Flow cytometry detected an increase in CD34-positive cells, suggestive of a blast population, but no blasts were observed in the peripheral blood. Clinically, there were no symptoms and blood values remained slightly low but stable.

In March 2017, the patient developed worsening pancytopenia with an Hgb of 8.8 g/dl, neutrophils at $0.5 \times 10^9/l$, and platelets $29 \times 10^9/l$. Peripheral blood analysis showed 1% blasts. A subsequent bone marrow biopsy revealed increasingly dysplastic megakaryocytes. G-banding again showed the t(17;19)(q21;p13) translocation in all examined metaphases. Molecular analysis at another laboratory found no pathogenic variants of tumor protein p53 (*TP53*). However, variants of the genes ASXL transcriptional regulator 1 (*ASXL1*, located on 20q11.21), tet methylcytosine dioxygenase 2 (*TET2*, 4q24), and DEAD-box helicase 41 (*DDX41*, 5q35.3), all of which are known to be involved in MDS pathogenesis (21), were found. The variants were: NM_015338.5(*ASXL1*):c.3977C>T (p.Pro1326Leu) with variant allele frequency (VAF) of 48.6%, NM_001127208.3(*TET2*):c.323A>T (p.Gln108>Leu) with VAF of 48.3%, and NM_016222.4(*DDX41*):c.992_994del; (p.Lys331del) with VAF of 45%.

A bone marrow transplant was recommended as the next line of treatment, but the patient opted against the procedure. Instead, Azacitidine was initiated for a duration of 5 days. Despite no complications, there was no improvement in hematologic values. Subsequent biopsy and cytogenetic evaluations in December 2017 showed no significant changes. In January 2018, an 8-week Melphalan treatment course, administered as a study drug, demonstrated a positive effect on all cell lines both in terms of measurements and morphology. The drug failed however to have any effect during a second course given in August 2018. Consequently, the patient was transferred to a palliative regimen involving blood transfusions and antibiotics when needed. She succumbed to a fungal infection in January 2019.

Patient 2. A 69-year-old woman, the younger sister of patient number 1, presented with a medical history of hypertension, type 2 diabetes mellitus, B12 deficiency, and an elevated BMI when referred in July 2019 for pancytopenia. Her hematologic values were Hgb 11.7 g/dl, MCV 111 fl, neutrophils $1.0 \times 10^9/l$, and platelets $75 \times 10^9/l$. A bone marrow biopsy showed features compatible with

MDS and 8% blasts. Hence, she was classified as having MDS-EB-1, close to EB-2. G-banding revealed an identical t(17;19)(q21;p13) as observed in Patient 1 in all 13 examined metaphases (see below for cytogenetic examination). The translocation was interpreted as a constitutional cytogenetic abnormality, later confirmed in a phytohemagglutinin (PHA)-stimulated blood sample. The variants NM_015338.5(*ASXL1*):c.3977C>T (p.Pro1326Leu) and NM_016222.4(*DDX41*):c.986AGA (p.Lys331del) were also identified and confirmed to be germline by testing of the oral mucosa.

In October 2019, the patient commenced Azacitidine treatment, resulting in a complete hematologic response. Hgb increased from 12.2 g/dl to 14.5 g/dl, neutrophils from $1.2 \times 10^9/l$ to $2.5 \times 10^9/l$, and thrombocytes from 69 to $255 \times 10^9/l$. However, over time the response declined, leading to the cessation of Azacitidine treatment in June 2023. In September 2023, Melphalan treatment was initiated due to severe pancytopenia (Hgb 6.6 g/dl, thrombocytes $6 \times 10^9/l$, neutrophils $0.38 \times 10^9/l$). A bone marrow biopsy in March 2023 showed 5% blasts and a slight increase in CD34+ cells. By September of the same year, the CD34-positive cell count had increased, suggesting a transition to acute myeloid leukemia (AML). Molecular pathology and cytogenetics were unchanged at this point. An 8-week course of Melphalan resulted in near normalization of CD34-positive cell levels and hematological values. Morphologically, the bone marrow showed improvement, with only mild dysplasia in thrombopoiesis. The latest hematologic values as of January 2024 showed a sustained positive response to the drug with an Hgb of 11.1 g/dl, platelets $131 \times 10^9/l$, and neutrophils $2.53 \times 10^9/l$.

G-banding analysis. Bone marrow and/or blood cells (Table I) were cytogenetically investigated using standard methods (22, 23); the cytogenetic examination of patient 2 also included analysis of a short-term culture of peripheral blood lymphocytes stimulated with phytohemagglutinin (PHA) for 72 h. Chromosome preparations were made from metaphase cells and G-banded using Leishman's stain (Sigma-Aldrich, St. Louis, Missouri, USA). Metaphases were analyzed and karyograms prepared using the CytoVision computer-assisted karyotyping system (Leica Biosystems, Newcastle upon Tyne, UK). The karyotype was written according to the International System for Human Cytogenomic Nomenclature (2020) (24).

Genomic DNA and total RNA isolation and synthesis of complementary DNA (cDNA). Genomic DNA was extracted from sample 2B (blood from patient 1) and sample 4 (bone marrow from patient 2; Table I) using a Maxwell RSC Instrument and the Maxwell RSC Tissue DNA Kit (Promega, Madison, WI, USA). The concentration was measured using Quantus Fluorometer and the QuantiFluor ONE dsDNA System (Promega).

Total RNA was extracted from sample 2B (blood from patient 1) and sample 3 (peripheral blood lymphocytes from patient 2 stimulated by PHA for 72 h) using the miRNeasy Mini Kit and QiaCube automated purification system according to the manufacturer's instructions (Qiagen, Hilden, Germany). The concentration was measured with the QIAxpert microfluidic UV/VIS spectrophotometer (Qiagen). RNA integrity was assessed with the Agilent 2100 bioanalyzer and DV200 index and found to be 76% (25). Complementary DNA (cDNA) was synthesized from 35 ng of total RNA in a 20 μ l reaction volume using iScript Advanced cDNA Synthesis Kit for RT-qPCR according to the manufacturer's instructions (Bio-Rad, Hercules, CA, USA).

Table I. Samples from patients 1 and 2 analyzed using G-banding karyotyping and molecular techniques.

Patient	Samples/ Type of cells ^a	Day (from sample 1)	Analysis ^b	Results
Patient 1	Sample 1/BM	0	G-banding	46,XX,t(17;19)(q21;p13)[3]
	Sample 2/BM	906	G-banding	46,XX,t(17;19)(q21;p13)[25]
	Sample 2B/BL	906	RT-PCR, gPCR, Sanger seq	<i>MYO1F::WNK4</i> and <i>VPS25::MYO1F</i> : Chimeric transcripts and genomic fragments. Deletions: chr17:40,928,500-40,934,435 and chr19:8,602,056-8,607,755 <i>MYO1F</i> variants: 6
	Sample 3/BM	1206	G-banding	46,XX,t(17;19)(q21;p13)[cp2]
Patient 2	Sample 1/BM	0	G-banding	46,XX,t(17;19)(q21-22;p13)[13]
	Sample 2/BM	867	G-banding	46,XX,t(17;19)(q21~22;p13)[11]
	Sample 3/PHA-BL	901	G-banding, RNA-seq, RT-PCR, Sanger seq	46,XX,t(17;19)(q21;p13)c <i>MYO1F::WNK4</i> and <i>VPS25::MYO1F</i> chimeric transcripts
	Sample 4/BM	1314	G-banding, gPCR, Sanger seq	46,XX,t(17;19)(q21;p13)c[20] <i>MYO1F::WNK4</i> and <i>VPS::MYO1F</i> : Chimeric genomic fragments Deletions: chr17:40,928,500-40,934,435 and chr19:8,602,056-8,607,755 <i>MYO1F</i> variants: 6
	Sample 5/BM	1483	G-banding	46,XX,t(17;19)(q21;p13)c[6]
	Sample 6/BM	1553	G-banding	46,XX,t(17;19)(q21;p13)c[25]
	Sample 7/BM	1616	G-banding	46,XX,t(17;19)(q21;p13)[cp5]

^aBM: Bone marrow; BL: blood; PHA-BL: peripheral blood lymphocytes stimulated by phytohemagglutinin (PHA) for 72 h. ^bRT-PCR: Reverse transcription-polymerase chain reaction; gPCR: genomic PCR; seq: sequencing.

RNA sequencing. Two hundred nanograms of total RNA extracted from peripheral blood lymphocytes from patient 2 (sample 3, Table I) were sent to the Genomics Core Facility at the Norwegian Radium Hospital, Oslo University Hospital for high-throughput paired-end RNA sequencing. A total of 50 million reads of 151-bp length were obtained. For quality control of the raw sequence data, the FASTQC software (available at <http://www.bioinformatics.babraham.ac.uk/projects/fastqc/>) was used. Fusion transcripts were found using the FusionCatcher software (26, 27).

Polymerase chain reaction (PCR) and Sanger sequencing analyses. The primers for the genes myosin IF (*MYO1F*), WNK lysine deficient protein kinase 4 (*WNK4*), and vacuolar protein sorting 25 homolog (*VPS25*) are described in Table II. For reverse transcription-polymerase chain reaction (RT-PCR) and cycle Sanger sequencing, the BigDye Direct Cycle Sequencing Kit was used (ThermoFisher Scientific, Waltham, MA, USA) according to the company's recommendations. The forward primers (F1) had the M13 forward primer sequence TGTAACGACGGCCAGT at their 5'-end whereas the reverse primers (R1) had the M13 reverse primer sequence CAGGAAACAGCTATGACC at their 5'-end. As template, cDNA corresponding to 2 ng total RNA was used. The primer combinations were M13For-MYO1F-1560F1/M13Rev-WNK4-800R1 and M13For-VPS25-371F1/M13Rev-MYO1F-1874R1 (Table II).

Nested PCR was used for amplification of the genomic *MYO1F::WNK4* and *VPS25::MYO1F* chimeric fragments. PCRs were performed in 25 µl reaction volume containing 12.5 µl Premix Ex Taq™ DNA Polymerase Hot Start Version (Takara Bio Europe/SAS,

Saint-Germain-en-Laye, France), template DNA, and 0.4 µM of each of the forward and reverse primers. For the outer PCR, the template was 60 ng of genomic DNA whereas for the nested PCR, the template was one microliter of the outer PCR products. For amplification of the genomic *MYO1F::WNK4* fragment, primer combinations MYO1F-intr14F1/WNK4-intr1R1 and MYO1F-intr14F2/WNK4-intr1-R2 were used for the outer and nested PCR, respectively. The PCR cycling conditions included an initial denaturation step at 94°C for 30 sec followed by 35 cycles of 7 sec at 98°C (denaturation step) and 3 min at 68°C (combined annealing and extension step), and a final extension for 5 min at 68°C. For amplification of the genomic *VPS25::MYO1F* fragment, primer combinations VPS25-Intr5F1/MYO1F-1881R1 and VPS25-Intr5F2/MYO1F-1856R1 were used for the outer and nested PCR, respectively. The PCR cycling conditions were as described above except that 2 min at 68°C was used.

Three microliters (3 µl) of the PCR products were stained with GelRed (Biotium, Fremont, CA, USA), analyzed by electrophoresis through 1.5% agarose gel, and photographed. DNA gel electrophoresis was performed using lithium borate buffer (28). The remaining PCR products were purified using the MinElute PCR Purification Kit (Qiagen) and direct sequenced using the dideoxy procedure with the BigDye Terminator v1.1 Cycle Sequencing Kit following the company's recommendations (ThermoFisher Scientific). Sequencing was run on the Applied Biosystems SeqStudio Genetic Analyzer system (ThermoFisher Scientific).

Bioinformatic analyses. The basic local alignment search tool (BLAST) was used to compare the sequences obtained by Sanger sequencing

Table II. Designation, sequence (5'→3'), and position in reference sequences of the forward (F1) and reverse (R1) primers used for polymerase chain reaction (PCR) amplification and Sanger sequencing analyses. M13 forward primer (*TGTAAAACGACGGCCAGT*) and M13 reverse primer (*CAGGAAACAGCTATGACC*) sequences are in bold and italics.

Designation	Sequence (5'→3')	Position on assembly GRCH37/hg19 (February 2009)
M13For-MYO1F-1560F1	<i>TGTAAAACGACGGCCAGT</i> ACC AGA CAC TGC TGC AGA AGC TGC	chr19:8,609,255-8,609,278
M13Rev-WNK4-800R1	<i>CAGGAAACAGCTATGACC</i> CTC AGC ACC GAC TTC CAC GAA TCA	chr17:40,934,868-40,934,891
M13For-VPS25-371F1	<i>TGTAAAACGACGGCCAGT</i> TTT CCA GGA GTG GCC AGA ACA ACT C	chr17:40,928,264-40,928,288
M13Rev-MYO1F-1874R1	<i>CAGGAAACAGCTATGACC</i> GTT GGG TTT GAT GCA GCG GAT GTA	chr19:8,601,868-8,601,891
MYO1F-intr14F1	ACT GTC CCC CGC CTC AAT CCA CC	chr19:8,609,027-8,609,049
WNK4-intr1R1	ACG GGT GTC ATG TCA GGC CCA GG	chr17:40,934,739-40,934,761
MYO1F-intr14F2	CCC TGA CCT CTG ATC CAG GCC ACA G	chr19:8,608,470-8,608,494
WNK4-intr1R2	CTT TAT GCA GCC CGG TCC CAG AGC	chr17:40,934,505-40,934,528
VPS25-Int4F1	TGG ATC AGA GGG GTG GAG CTG ATG AA	chr17:40,928,178-40,928,203
MYO1F-1881R1	CTT GGT CTC GTT GGG TTT GAT GCA GC	chr19:8,601,859-8,601,884
VPS25-Int4F2	TTC ACA GGT TTC CAG GAG TGG CCA GA	chr17:40,928,256-40,928,281
MYO1F-1856R1	CGG ATG TAG TGG GGT GTG CAC CTC AT	chr19:8,601,884-8,601,909
WNK-intr1R6	TCC CAG AGC CCT GAG CTC AAT AG	chr17:40,934,491-40,934,513
MYO1F-intr14F7*	GGC ACC TGT AAT CCC AGC TAC TCA	chr19:8,607,912-8,607,935
MYO1F-intr14F8*	GCT GAG GCA GGA GAA TCA CTT GAA	chr19:8,607,884-8,607,907

*Used only for the Sanger sequencing of the genomic *MYO1F::WNK4* amplified fragments

with the NCBI reference sequences NM_012335.4, NG_052844.1 (*MYO1F*), NM_032387.5, NG_016227.1 (*WNK4*), NM_032353.4, and AC100793.8 (*VPS25*) (29). The BLAT alignment tool and the human genome browser at University of California, Santa Cruz (UCSC) were also used to map the sequences on the Human GRCh37/hg19 assembly (30, 31). The single nucleotide polymorphism database (dbSNP, at <https://www.ncbi.nlm.nih.gov/snp/>) and genome aggregation database (gnomAD v2.1.1 at <https://gnomad.broadinstitute.org/>) were used for nucleotide sequence variation. A search for conserved domains (CD) within amino acids sequences (32-34) was performed using the CD-search on line program (<https://www.ncbi.nlm.nih.gov/Structure/cdd/wrpsb.cgi>) and ScanProsite tool (<https://prosite.expasy.org/scanprosite/>).

Results

G-banding analyses. Cytogenetic examination of short-term cultured cells revealed a balanced t(17;19)(q21;p13) in all metaphase cells studied. The translocation was thus present in all three samples from patient 1 and all seven samples from patient 2, including the sample containing PHA-stimulated lymphocytes (Table I, Figure 1).

RNA-sequencing and molecular genetic confirmation of fusion transcripts. Analysis of the RNA sequencing data using the FusionCatcher software detected two *MYO1F::WNK4* chimeric transcripts (types 1 and 2) and a single *VPS25::MYO1F* transcript attributable to the reciprocal t(17;19)(q21;p13) translocation (Table III). In the *MYO1F::WNK4* type 1 transcript, exon 14 of *MYO1F* (reference sequence NM_012335.4) was fused in-frame to exon 2 of *WNK4* (reference sequence NM_032387.5). In the

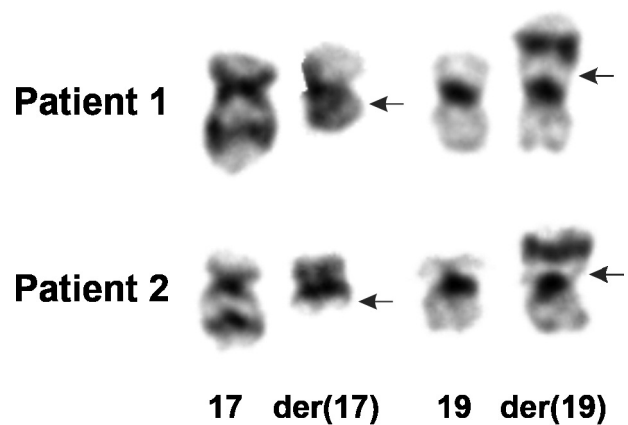


Figure 1. G-banding analysis of short-term cultured cells from sample 2/bone marrow of patient 1 and sample 3/peripheral blood lymphocytes stimulated by phytohemagglutinin (PHA) for 72 h of patient 2. Partial karyograms showing the der(17)t(17;19)(q21;p13) and der(19)t(17;19)(q21;p13) together with the corresponding normal chromosome homologs; breakpoint positions are indicated by arrows.

type 2 transcript, exon 12 *MYO1F* was fused in-frame to exon 2 of *WNK4*. In the *VPS25::MYO1F* transcript, finally, exon 5 of *VPS25* (NM_032353.4) was fused out-of-frame to exon 17 of *MYO1F* (NM_012335.4).

The presence of the *MYO1F::WNK4* type 1 and *VPS25::MYO1F* chimeric transcripts was verified in peripheral blood lymphocytes from both patients using RT-PCR and cycle Sanger sequencing (Table I, Figure 2 and Figure 3). No

Table III. The *MYO1F::WNK4* and *VPS25::MYO1F* chimeric transcripts detected in blood cells from patient 2 after analysis of RNA sequencing data with FusionCatcher. Exons are based on the reference sequences NM_012335.4 for *MYO1F*, NM_032387.5 for *WNK4*, and NM_032353.4 for *VPS25*.

Fusion transcript	Fusion sequence
<i>MYO1F::WNK4</i> (exon 14-exon 2)	CAGCTGGAGCGCCGGCTTCGTCATCCACCACTACGCTGGCAAG:: ACTCGGAAACTGTCTAGAGCTGAGCGGCAGCGCTTCTCAGAGG
<i>MYO1F::WNK4</i> (exon 12-exon 2)	GCTGCAGCAAATCTTATCGAACTACCCTGAAGGCCGAGCAG:: ACTCGGAAACTGTCTAGAGCTGAGCGGCAGCGCTTCTCAGAGG
<i>VPS25::MYO1F</i> (exon 5-exon 17)	ACCCTGTATGAACTGACTAATGGGGAAGACACAGAGGATGAGG:: AAACAAGCCAACGACCTGGTGGCCACACTGATGAGGTGCACAC

attempts were made to amplify the *MYO1F::WNK4* type 2 chimeric transcript. Analysis using the BigDye Direct Cycle Sequencing Kit with the primer combination M13For-MYO1F-1560F1/M13Rev-WNK4-800R1 confirmed the in-frame fusion of exon 14 of *MYO1F* with exon 2 of *WNK4* (*MYO1F::WNK4* type 1, Figure 2A). Based on the reference sequences NM_012335.4/NP_036467.2 (*MYO1F*) and NM_032387.5/NP_115763.2 (*WNK4*), the *MYO1F::WNK4* chimeric transcript 1 codes for a 1545 amino acid long putative protein consisting of the first 508 amino acids of MYO1F and amino acids 207-1243 from *WNK4* (Figure 2B).

Analyses using the BigDye Direct Cycle Sequencing Kit with the primer combination M13For-VPS25-371F1/M13Rev-MYO1F-1874R1 confirmed the out-of-frame fusion of exon 5 of *VPS25* with exon 17 of *MYO1F* (*VPS25::MYO1F* transcript, Figure 3A). Based on the reference sequences NM_032353.4/NP_115729.1 (*VPS25*) and the above-mentioned reference sequences for *MYO1F*, the *VPS25::MYO1F* chimeric transcript is predicted to encode a 376 amino acid peptide consisting of the first 140 amino acids of *VPS25* and 236 amino acids from the out-of-frame *MYO1F* exons (Figure 3B). Our analysis using the NCBI Conserved Domain Search and ScanProsite tool showed that the 236 amino acids do not contain any known conserved domain.

Identification of the MYO1F::WNK4 and VPS25::MYO1F genomic breakpoints. Nested PCR using *MYO1F*-forward and *WNK4*-reverse primers, conducted on extracted DNA from the blood of patient 1 (sample 2B) and bone marrow of patient 2 (sample 4), amplified genomic fragments in both cases (Figure 4A). Sequencing of the PCR fragments showed that they had identical genomic fusion points occurring in intron 14 of *MYO1F* and intron 2 of *WNK4* (Figure 4B). Nested PCR with *VPS25*-forward and *MYO1F*-reverse primers using the above-mentioned template DNAs also amplified genomic fragments (Figure 4A). Sequencing of these PCR fragments showed that they were genomic chimeric fragments with identical fusion points in introns 5 of *VPS25* and 16 of *MYO1F* (Figure 4C). A four-nucleotide CAGC overlap was found in the junction between the two genes (Figure 4C).

The identification of *MYO1F::WNK4* and *VPS25::MYO1F* genomic breakpoints also showed that the apparently balanced t(17;19)(q21;p13) chromosomal translocation was accompanied by sub-microscopic deletions on both chromosomes (Figure 4B-D). On chromosome 17, a 6 Kbp deletion was found, starting in intron 5 of *VPS25* and ending in intron 1 of *WNK4* (chr17:40,928,500-40,934,435) (Figure 4D). On chromosome 19, a 5.7 Kbp deletion was detected, starting in intron 16 of *MYO1F* and ending in intron 14 of that gene (chr19:8,602,056-8,607,755) (Figure 4D).

In addition, the sequence alignment of the genomic PCR fragments with the reference sequence NG_052844.1 (*MYO1F*) revealed the presence of identical intronic variants in the *MYO1F* locus in both patients, indicating that the same *MYO1F* allele was involved in the translocation (Table IV). We did not search for variants (single nucleotide variants, SNP) in the *VPS25* and *WNK4* loci.

Discussion

We report the finding of a novel constitutional chromosomal translocation, t(17;19)(q21;p13), in bone marrow cells as well as PHA-stimulated peripheral blood lymphocytes from two siblings with MDS. The siblings were not twins - they had an age difference of 45 months - so it is highly likely that they inherited the translocation from a carrier parent. The parents are dead, and it has not been possible to conduct relevant genetic investigations on any other family members. Hence, we do not know whether other carriers exist that do not suffer from any bone marrow disease.

In our view, the found translocation probably predisposed the two individuals to MDS development; indeed, it may represent an initial step in leukemogenesis, more or less in accordance with Knudson's hypothesis (35). What we do know is that the t(17;19)(q21;p13) rearranged three genes - *MYO1F* (on 19p13), *WNK4*, and *VPS25* (both latter loci are on 17q21) - resulting in the creation of two novel chimeras, *MYO1F::WNK4* and *VPS25::MYO1F*. This, in turn, in all likelihood led to abnormal function of the said genes. Because the same intronic variants in *MYO1F* were present

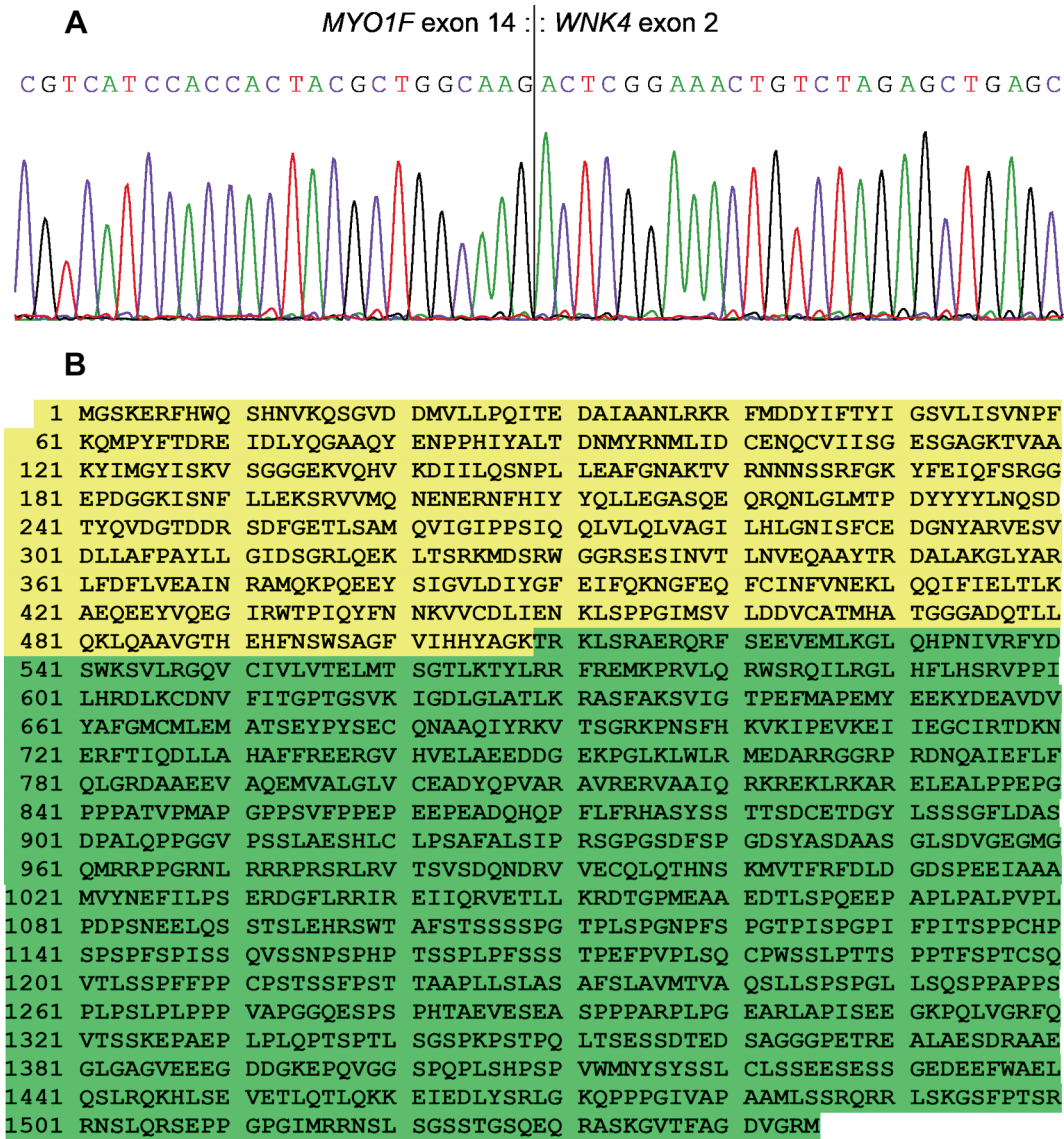


Figure 2. Confirmation of the *MYO1F::WNK4* type 1 chimeric transcript with reverse transcription-polymerase chain reaction (RT-PCR) and cycle Sanger sequencing. (A) Partial sequence chromatogram of the cDNA amplified fragment showing the fusion of exon 14 of *MYO1F* (reference sequence NM_012335.4) to exon 2 of *WNK4* (reference sequence NM_02387.5). The *MYO1F::WNK4* type 1 chimeric transcript was found in RNA extracted from sample 2/blood of patient 1 and sample 3/peripheral blood lymphocytes stimulated by phytohemagglutinin (PHA) for 72 h of patient 2. (B) The 1545 amino acid residues of the *MYO1F::WNK4* protein consist of the first 508 amino acids (in yellow) of *MYO1F* (1-508 from NP_036467.2) and the last 1,037 amino acids (in green) from *WNK4* (207-1243 from NP_115763.2).

near the genetic breakpoints in both patients, we believe that the same inherited *MYO1F* allele was involved in the translocation in both. Furthermore, it turned out that the t(17;19)(q21;p13) was not truly balanced but instead was accompanied by submicroscopic deletions on chromosomes 17 and 19, identical in both siblings. Thus, the analysis of the genomic breakpoint (at the level of DNA) unequivocally indicates a common ancestry for the translocation. Since the three genes *MYO1F*, *WNK4*, and *VPS25* are transcribed from

centromere to telomere, we predict that the translocation led to formation of a *MYO1F::WNK4* on the der(19)t(17;19)(q21;p13), whereas a *VPS25::MYO1F* was formed on the der(17)t(17;19)(q21;p13).

MYO1F codes for the myosin IF (*MYO1F*) protein which is a long-tailed unconventional class I myosin (Figure 5) (36-38). The *MYO1F* gene is expressed in blood and immune cells with high levels of expression in NK-cells, Kupffer cells, monocytes, macrophages, Hofbauer cells, and T-cells (39-41).

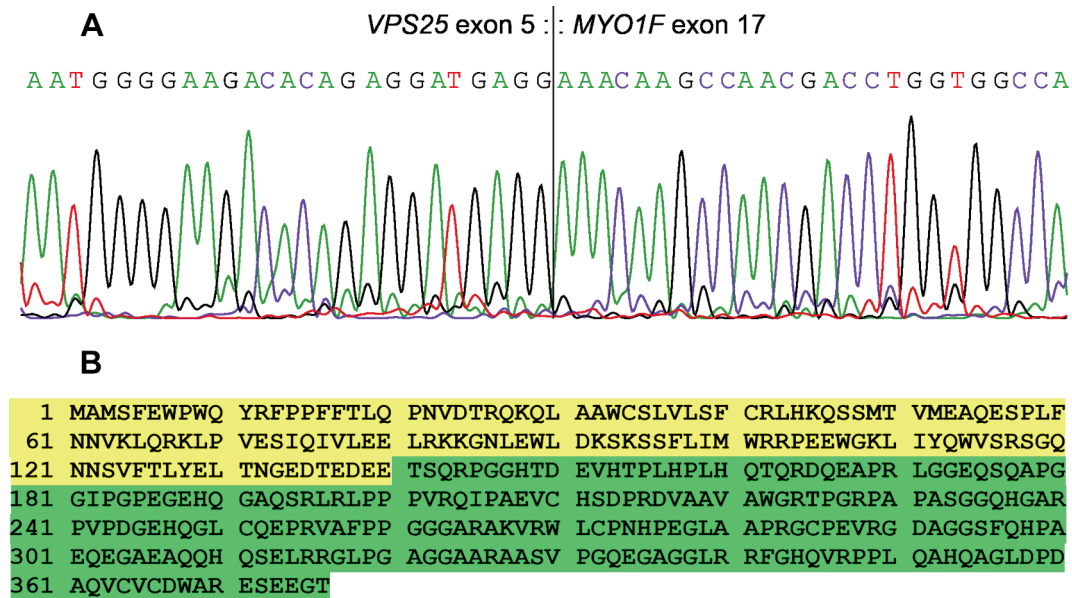


Figure 3. Confirmation of the *VPS25::MYO1F* chimeric transcript with reverse transcription-polymerase chain reaction (RT-PCR) and cycle Sanger sequencing. (A) Partial sequence chromatogram of the cDNA amplified fragment showing the fusion of exon 5 of *VPS25* (reference sequence NM_032353.4) to exon 17 of *MYO1F* (reference sequence NM_012335.4). The *VPS25::MYO1F* chimeric transcript was found in RNA extracted from sample 2/blood of patient 1 and sample 3/peripheral blood lymphocytes stimulated by phytohemagglutinin (PHA) for 72 h of patient 2. (B) The putative 376 amino acid peptide coding product of the *VPS25::MYO1F* chimeric transcript. The peptide is composed of the first 140 amino acids (in yellow) from *VPS25* (NP_115729.1) and 236 amino acids (green) from the out-of-frame fused *MYO1F* (exons 17 to 28) (NM_012335.4).

MYO1F is a motor protein that utilizes the energy generated by hydrolysis of adenosine triphosphate (ATP) to move along actin filaments. At its N-terminal part lies a motor domain (region 11-677 in reference sequence NP_036467.2) containing the binding site for ATP and hydrolysis, as well as the binding site for actin. This is followed by an IQ motif, a binding site for different proteins containing EF-hand calcium-binding motifs (region 697-722 in NP_036467.2), a pleckstrin homology (PH)/basic tail homology 1 (TH1) domain capable of binding to lipid membranes (region 717-917 in NP_036467.2), and a Src homology 3 (SH3) domain at the C-terminus which binds to proline rich regions and is involved in protein-protein interactions (region 1041-1098 in NP_036467.2) (Figure 5).

MYO1F has been reported to be a 3'-end partner gene in two recurrent in-frame chimeras found in neoplastic disorders. In infant acute myeloid leukemias, exon 9 of the lysine methyltransferase 2A gene (*KMT2A*, also known as *MLL*, reference sequence NM_005933.4) fuses in-frame to exon 2 of *MYO1F* (*KMT2A::MYO1F*) (42, 43). In peripheral T-cell lymphomas not otherwise specified (PTCL-NOS), exon 25 of the vav guanine nucleotide exchange factor 1 gene (*VAV1*, reference sequence NM_005428.4) fuses to exon 25 of *MYO1F* (44). The oncogenicity of the *VAV1::MYO1F* chimera has been demonstrated in murine models (45, 46).

WNK4 codes for a serine-threonine protein kinase (Figure 5), one of four members of the lysine deficient (WNK) serine-threonine protein kinases [WNK is an initialism for With No lysine (K)] (47-49). *WNK4* is mainly expressed in the distal convoluted tubule (DCT) and cortical collecting duct (CCD) of the kidney (40, 41, 50). Pathogenic sequence variants of *WNK4* have been reported to cause type IIB pseudohypoadosteronism (PHA2B), an autosomal dominant condition characterized by hypertension, hyperkalemia, and hyperchloremic metabolic acidosis (49-53). The *WNK4* protein accumulates exclusively in intercellular junctions in DCT, but also in the cytoplasm in CCD. The protein is considered to be a master kinase regulating thiazide-sensitive $\text{Na}^+\text{-Cl}^-$ cotransporter (NCC) (49, 50, 53-56). *WNK4* activates the oxidative stress responsive kinase 1 (OXSR1) and serine/threonine kinase 39 (STK39, also known as STE20/SPS1-related proline/alanine-rich kinase, SPAK, and PASK) to modulate cotransporter activity (49, 53-57). According to the database of protein disorders and mobility annotations (MobiDB), only 37% of the protein has a secondary structure, whereas 63% of the primary amino acid sequence of *WNK4* is intrinsically disordered (<https://mobidb.org/Q96J92>) (58). Intrinsically disordered regions play important roles in a plethora of cellular functions (59-62). In protein kinases, intrinsically disordered regions may interact

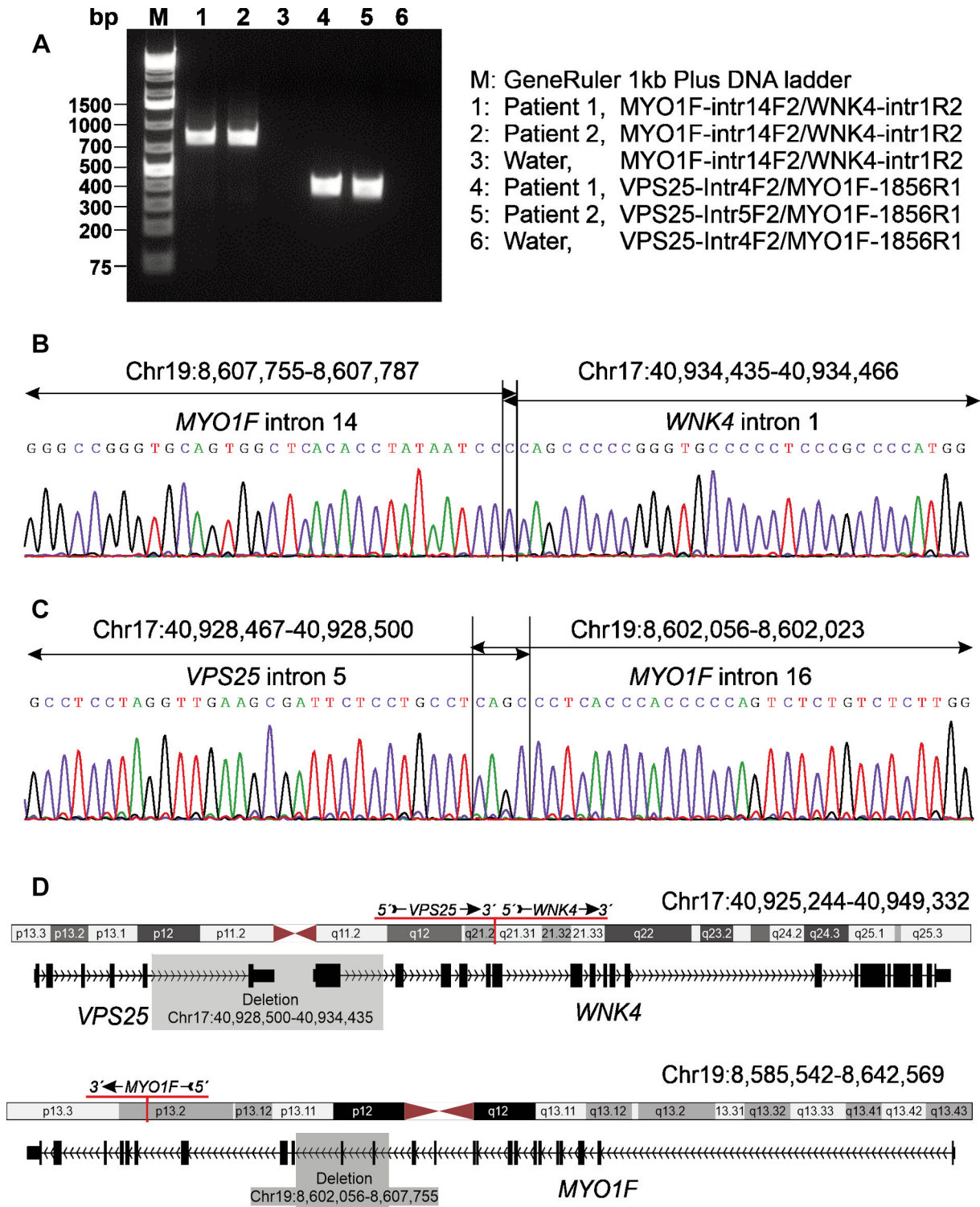


Figure 4. Identification of the MYO1F::WNK4 and VPS25::MYO1F genomic breakpoints. (A) Gel electrophoresis showing the genomic PCR amplified fragments found in extracted DNA from sample 2/blood of patient 1 and sample 4/bone marrow of patient 2. (B) Partial sequence chromatogram showing the fusion of a sequence from intron 14 of MYO1F with a sequence from intron 1 of WNK4. (C) Partial sequence chromatogram showing the fusion of a sequence from intron 5 of VPS25 with a sequence from intron 16 of MYO1F. (D) Ideograms of chromosomes 17 and 19 (not in scale) showing the positions and orientations of the transcription of the VPS25, WNK4, and MYO1F genes. The submicroscopically deleted regions accompanying the t(17;19)(q21;p13) are in grey.

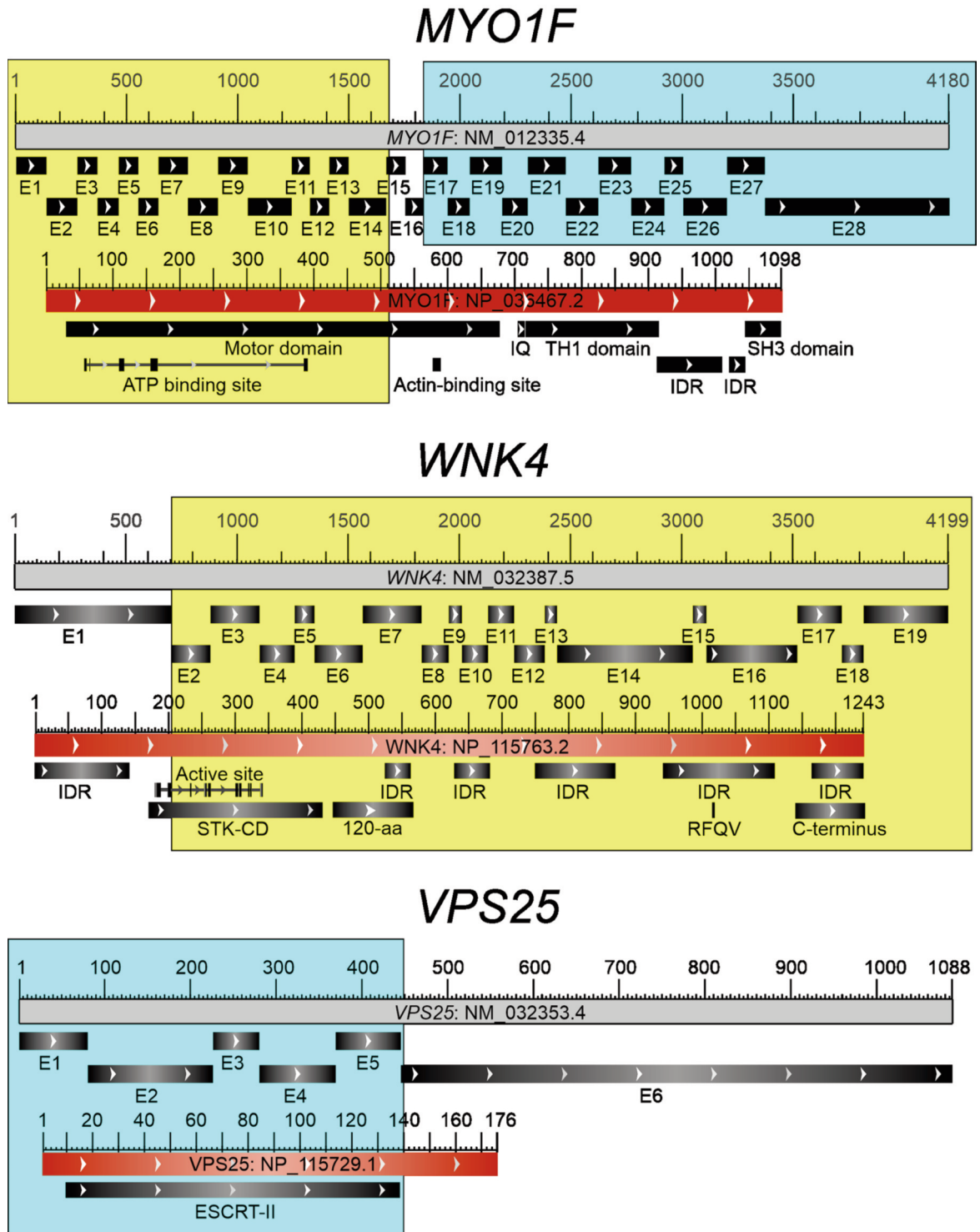


Figure 5. Illustration showing mRNA and coding proteins of the genes myosin IF (*MYO1F*), WNK lysine deficient protein kinase 4 (*WNK4*), and vacuolar protein sorting 25 homolog (*VPS25*). They are rearranged by the t(17;19)(q21;p13) chromosomal translocation and forming *MYO1F::WNK4* (yellow) and *VPS25::MYO1F* (cyan) chimeras. E: Exon; IQ: IQ motif; TH1 domain: pleckstrin homology (PH)/basic tail homology 1 (TH1) domain; SH3 domain: Src homology 3 domain; IDR: intrinsically disordered region; STK-CD: serine/threonine protein kinase catalytic domain; 120-aa: region of 120 amino acids which includes an oxidative-stress-responsive kinase 1 C-terminal domain, autoinhibitory domain, a coiled-coil domain (CCD) and an acidic motif; RFQV: serine/threonine kinase 39 (STK39) binding site; C-terminus: carboxyl-terminal region containing several functional domains, including binding sites for calmodulin and protein phosphatase 1; ESCRT-II: endosomal sorting complex required for transport -II (ESCRT-II complex) subunit.

Table IV. Intronic variants detected in both patients close to the genomic breakpoints in *MYO1F*.

Genome Aggregation Database (gnomAD) v2.1.1 (GRCh37)	Detected allele
SNV:19-8602027-T-G	G
Insertion (2 bases):19-8601958-C-CAG	insAG
SNV:19-8607766-C-T	T
SNV: 19-8607949-G-A	A
SNV: 19- 8608013-C-G	G
SNV: 19-8608040- A-G	G

with and regulate the kinase domain (63-65). The catalytic domain of the serine/threonine protein kinase spans from amino acids 172 to 432 in the reference sequence NP_115763.2. This domain is followed by a region of approximately 120 amino acids (between amino acids 450-570 in NP_115763.2) that includes an autoinhibitory domain, a coiled-coil domain and an acidic motif, as well as a conserved RFQV motif (aa 1016-1019) which serves as an STK39 binding site (49, 57). Additionally, there is a carboxyl-terminal region (amino acids 1140-1243) containing several functional domains, including binding sites for calmodulin and protein phosphatase1 (49, 66) (Figure 5).

VPS25 encodes a protein that is part of the endosomal sorting complex required for transport (ESCRT) (Figure 5). Two molecules of *VPS25* (also known as *EAP20*) together with one molecule of *SNF8* (also known as *EAP30*) and one molecule of *VPS36* (also known as *EAP45*) form the ESCRT-II complex that is involved in endocytosis of ubiquitinated membrane proteins (67, 68). Additionally, *VPS25*, *VPS36*, and *SNF8* may form a multiprotein complex with the RNA polymerase II elongation factor proteins of *ELL* (69-72).

The chimeric *MYO1F::WNK4* gene generated by the 17;19-translocation is predicted to code for a chimeric serine/threonine kinase (Figure 5). This comprises the N-terminal part the *MYO1F* protein, which contains the binding site for ATP and hydrolysis, and part of the *WNK4* protein that includes the catalytic domain of the serine/threonine protein kinase and all subsequent functional regions of *WNK4* (autoinhibitory and coiled-coil domains, acidic and RFQV motifs, the binding sites for calmodulin and protein phosphatase 1, and other functional domains at the carboxyl-terminus). Deregulation of kinases, including serine/threonine kinases, is a well-known oncogenetic mechanism and inhibitors of deregulated kinases are a major modality in anti-cancer pharmacology (73-79).

The chimeric *VPS25::MYO1F* transcript would code for an abnormal *VPS25* protein (Figure 5) containing the part of the wild-type or normal *VPS25* protein that codes for the ESCRT-

II complex subunit, along with an additional 236 amino acids derived from the out-of-frame fused *MYO1F* exons. Detailed studies are required to understand the cellular role of this abnormal protein and how these 236 amino acids affect the function of the ESCRT-II complex subunit.

In conclusion, we describe a novel constitutional chromosomal translocation, t(17;19)(q21;p13), in two sisters with MDS, suggesting a genetic predisposition for this bone marrow neoplasia. The translocation involved three genes - *MYO1F*, *WNK4*, and *VPS25* - and created two chimeras. The abnormal fusion genes, *MYO1F::WNK4* and *VPS25::MYO1F*, probably played a crucial role in MDS pathogenesis. This is particularly likely for *MYO1F::WNK4* since the protein product of this chimera was an abnormal serine/threonine kinase. Further studies are needed to understand the cellular implications of these chimeric genes, whether they are involved also in sporadic MDS cases, and whether the finding of such fusions could be used therapeutically.

Conflicts of Interest

The Authors declare that they have no potential conflicts of interest.

Authors' Contributions

IP designed and supervised the research, performed molecular genetic experiments, bioinformatics analysis, interpreted the data, and wrote the manuscript. KA performed G-banding, karyotyping, molecular genetic experiments, and interpreted the data. VS made clinical evaluations and treated the patients. ST made clinical evaluations. SH assisted with cytogenetics and writing of the manuscript. MRT evaluated cytogenetic data and assisted with writing of the manuscript. All Authors read and approved of the final manuscript.

Acknowledgements

This project was financial supported by internal funding program of the Institute for Cancer Genetics and Informatics.

References

- 1 Heim S, Mitelman F: Chromosome abnormalities in the myelodysplastic syndromes. *Clin Haematol* 15(4): 1003-1021, 1986.
- 2 Heim S, Mitelman F: Cytogenetic analysis in the diagnosis of acute leukemia. *Cancer* 70(6 Suppl): 1701-1709, 1992. DOI: 10.1002/1097-0142(19920915)70:4+<1701::aid-encr2820701609>3.0.co;2-s
- 3 Heim S, Mitelman F: *Cancer Cytogenetics: Chromosomal and molecular genetic aberrations of tumor cells*. Fourth Edition edn. Wiley-Blackwell, 2015.
- 4 Panagopoulos I, Heim S: Interstitial deletions generating fusion genes. *Cancer Genomics Proteomics* 18(3): 167-196, 2021. DOI: 10.21873/cgp.20251
- 5 Panagopoulos I, Andersen K, Gorunova L, Lund-Iversen M, Lobmaier I, Heim S: Recurrent fusion of the genes for high-

- mobility group AT-hook 2 (*HMGA2*) and nuclear receptor co-repressor 2 (*NCOR2*) in osteoclastic giant cell-rich tumors of bone. *Cancer Genomics Proteomics* 19(2): 163-177, 2022. DOI: 10.21873/cgp.20312
- 6 Rowley JD: The critical role of chromosome translocations in human leukemias. *Annu Rev Genet* 32(1): 495-519, 1998. DOI: 10.1146/annurev.genet.32.1.495
- 7 Rowley JD: The role of chromosome translocations in leukemogenesis. *Semin Hematol* 36(4 Suppl 7): 59-72, 1999.
- 8 Welborn J: Constitutional chromosome aberrations as pathogenic events in hematologic malignancies. *Cancer Genet Cytogenet* 149(2): 137-153, 2004. DOI: 10.1016/s0165-4608(03)00301-7
- 9 Panani AD: Is there an association with constitutional structural chromosomal abnormalities and hematologic neoplastic process? A short review. *Ann Hematol* 88(4): 293-299, 2009. DOI: 10.1007/s00277-008-0672-8
- 10 Alimena G, Billström R, Casalone R, Gallo E, Mitelman F, Pasquali F: Cytogenetic pattern in leukemic cells of patients with constitutional chromosome anomalies. *Cancer Genet Cytogenet* 16(3): 207-218, 1985. DOI: 10.1016/0165-4608(85)90047-0
- 11 Benítez J, Valcarcel E, Ramos C, Ayuso C, Cascos AS: Frequency of constitutional chromosome alterations in patients with hematologic neoplasias. *Cancer Genet Cytogenet* 24(2): 345-354, 1987. DOI: 10.1016/0165-4608(87)90117-8
- 12 Hinoda Y, Itoh H, Takahashi T, Adachi M, Tsujisaki M, Imai K, Yachi A: Myelodysplastic syndrome in a patient with a unique constitutional chromosome abnormality t(2;11) (q31;p13). *Int J Hematol* 56(1): 95-97, 1992.
- 13 Smith SE, Joseph A, Nadeau S, Shridhar V, Gemmill R, Drabkin H, Knuutila S, Smith DI: Cloning and characterization of the human t(3;6)(p14;p11) translocation breakpoint associated with hematologic malignancies. *Cancer Genet Cytogenet* 71(1): 15-21, 1993. DOI: 10.1016/0165-4608(93)90197-t
- 14 Johnson EJ, Scherer SW, Osborne L, Tsui LC, Oscier D, Mould S, Cotter FE: Molecular definition of a narrow interval at 7q22.1 associated with myelodysplasia. *Blood* 87(9): 3579-3586, 1996.
- 15 Cerretini R, Acevedo S, Chena C, Belli C, Larripa I, Slavutsky I: Evaluation of constitutional chromosome aberrations in hematologic disorders. *Cancer Genet Cytogenet* 134(2): 133-137, 2002. DOI: 10.1016/s0165-4608(01)00621-5
- 16 Hill AS, MacCallum PK, Young BD, Lillington DM: Molecular cloning of a constitutional (7;22) translocation associated with risk of hematological malignancy. *Genes Chromosomes Cancer* 38(3): 260-264, 2003. DOI: 10.1002/gcc.10277
- 17 Ganly P, McDonald M, Spearing R, Morris CM: Constitutional t(5;7)(q11;p15) rearranged to acquire monosomy 7q and trisomy 1q in a patient with myelodysplastic syndrome transforming to acute myelocytic leukemia. *Cancer Genet Cytogenet* 149(2): 125-130, 2004. DOI: 10.1016/j.cancergencyto.2003.07.006
- 18 Gahrton C, Nahi H, Jansson M, Wallblom A, Alici E, Sutlu T, Samuelsson J, Gahrton G: Constitutional inv(3) in myelodysplastic syndromes. *Leuk Res* 34(12): 1627-1629, 2010. DOI: 10.1016/j.leukres.2010.05.014
- 19 Järviäho T, Bang B, Zachariadis V, Taylan F, Moilanen J, Möttönen M, Smith CIE, Harila-Saari A, Niinimäki R, Nordgren A: Predisposition to childhood acute lymphoblastic leukemia caused by a constitutional translocation disrupting *ETV6*. *Blood Adv* 3(18): 2722-2731, 2019. DOI: 10.1182/bloodadvances.2018028795
- 20 Lovatell VL, Bueno AP, Kós EAA, Meyer LGC, Ferreira GM, Kalonji MF, Mello FV, Milito CB, Costa ESD, Abdelhay E, Redondo MDT, Pombo-de-Oliveira MS, Fernandez TS: A novel constitutional t(3;8)(p26;q21) and *ANKRD26* and *SRP72* variants in a child with myelodysplastic neoplasm: clinical implications. *J Clin Med* 12(9): 3171, 2023. DOI: 10.3390/jcm12093171
- 21 Hosono N: Genetic abnormalities and pathophysiology of MDS. *Int J Clin Oncol* 24(8): 885-892, 2019. DOI: 10.1007/s10147-019-01462-6
- 22 Czepulkowski B: Basic techniques for the preparation and analysis of chromosomes from bone marrow and leukaemic blood. *In: Human cytogenetics: malignancy and acquired abnormalities*. Rooney DE (ed.). New York, Oxford University Press, pp. 1-26, 2001.
- 23 Potter AM, Watmore A: Cytogenetics in myeloid leukaemia. *In: Human cytogenetics: malignancy and acquired abnormalities*. Rooney DE (ed.). New York, Oxford University Press, pp. 27-55, 2001.
- 24 McGowan-Jordan J, Hastings RJ, Moore S: *ISCN 2020: An International system for human cytogenomic nomenclature*. Basel, Karger, pp. 164, 2020.
- 25 Matsubara T, Soh J, Morita M, Uwabo T, Tomida S, Fujiwara T, Kanazawa S, Toyooka S, Hirasawa A: DV200 index for assessing RNA integrity in next-generation sequencing. *Biomed Res Int* 2020: 9349132, 2020. DOI: 10.1155/2020/9349132
- 26 Kangaspeska S, Hultsch S, Edgren H, Nicorici D, Murumägi A, Kallioniemi O: Reanalysis of RNA-sequencing data reveals several additional fusion genes with multiple isoforms. *PLoS One* 7(10): e48745, 2012. DOI: 10.1371/journal.pone.0048745
- 27 Nicorici D, Satalan H, Edgren H, Kangaspeska S, Murumagi A, Kallioniemi O, Virtanen S, Kikku O: FusionCatcher – a tool for finding somatic fusion genes in paired-end RNA-sequencing data. *bioRxiv*, 2014. DOI:10.1101/011650
- 28 Singhal H, Ren YR, Kern SE: Improved DNA electrophoresis in conditions favoring polyborates and lewis acid complexation. *PLoS One* 5(6): e11318, 2010. DOI: 10.1371/journal.pone.0011318
- 29 Altschul SF, Gish W, Miller W, Myers EW, Lipman DJ: Basic local alignment search tool. *J Mol Biol* 215(3): 403-410, 1990. DOI: 10.1016/S0022-2836(05)80360-2
- 30 Kent WJ: BLAT – the BLAST-like alignment tool. *Genome Res* 12(4): 656-664, 2002. DOI: 10.1101/gr.229202
- 31 Kent WJ, Sugnet CW, Furey TS, Roskin KM, Pringle TH, Zahler AM, Haussler D: The human genome browser at UCSC. *Genome Res* 12(6): 996-1006, 2002. DOI: 10.1101/gr.229102
- 32 Wang J, Chitsaz F, Derbyshire MK, Gonzales NR, Gwadz M, Lu S, Marchler GH, Song JS, Thanki N, Yamashita RA, Yang M, Zhang D, Zheng C, Lanczycki CJ, Marchler-Bauer A: The conserved domain database in 2023. *Nucleic Acids Res* 51(D1): D384-D388, 2023. DOI: 10.1093/nar/gkac1096
- 33 de Castro E, Sigrist CJ, Gattiker A, Bulliard V, Langendijk-Genevaux PS, Gasteiger E, Bairoch A, Hulo N: ScanProsite: detection of PROSITE signature matches and ProRule-associated functional and structural residues in proteins. *Nucleic Acids Res* 34(Web Server issue): W362-W365, 2006. DOI: 10.1093/nar/gkl124
- 34 Sigrist CJ, de Castro E, Cerutti L, Cuche BA, Hulo N, Bridge A, Bougueleret L, Xenarios I: New and continuing developments at PROSITE. *Nucleic Acids Res* 41(Database issue): D344-D347, 2013. DOI: 10.1093/nar/gks1067
- 35 Knudson AG Jr, Hethcote HW, Brown BW: Mutation and childhood cancer: a probabilistic model for the incidence of retinoblastoma. *Proc Natl Acad Sci USA* 72(12): 5116-5120, 1975. DOI: 10.1073/pnas.72.12.5116

- 36 Maravillas-Montero JL, Santos-Argumedo L: The myosin family: unconventional roles of actin-dependent molecular motors in immune cells. *J Leukoc Biol* 91(1): 35-46, 2011. DOI: 10.1189/jlb.0711335
- 37 Girón-Pérez DA, Piedra-Quintero ZL, Santos-Argumedo L: Class I myosins: Highly versatile proteins with specific functions in the immune system. *J Leukoc Biol* 105(5): 973-981, 2019. DOI: 10.1002/jlb.1mr0918-350rrr
- 38 Navinés-Ferrer A, Martín M: Long-tailed unconventional class I myosins in health and disease. *Int J Mol Sci* 21(7): 2555, 2020. DOI: 10.3390/ijms21072555
- 39 Kim SV, Mehal WZ, Dong X, Heinrich V, Pypaert M, Mellman I, Dembo M, Mooseker MS, Wu D, Flavell RA: Modulation of cell adhesion and motility in the immune system by Myo1f. *Science* 314(5796): 136-139, 2006. DOI: 10.1126/science.1131920
- 40 Uhlén M, Fagerberg L, Hallström BM, Lindskog C, Oksvold P, Mardinoglu A, Sivertsson Å, Kampf C, Sjöstedt E, Asplund A, Olsson I, Edlund K, Lundberg E, Navani S, Szgyarto CA, Odeberg J, Djureinovic D, Takanen JO, Hober S, Alm T, Edqvist PH, Berling H, Tegel H, Mulder J, Rockberg J, Nilsson P, Schwenk JM, Hamsten M, von Feilitzen K, Forsberg M, Persson L, Johansson F, Zwahlen M, von Heijne G, Nielsen J, Pontén F: Tissue-based map of the human proteome. *Science* 347(6220): 1260419, 2015. DOI: 10.1126/science.1260419
- 41 Karlsson M, Zhang C, Méar L, Zhong W, Digre A, Katona B, Sjöstedt E, Butler L, Odeberg J, Dusart P, Edfors F, Oksvold P, von Feilitzen K, Zwahlen M, Arif M, Altay O, Li X, Ozcan M, Mardinoglu A, Fagerberg L, Mulder J, Luo Y, Ponten F, Uhlén M, Lindskog C: A single-cell type transcriptomics map of human tissues. *Sci Adv* 7(31): eabh2169, 2021. DOI: 10.1126/sciadv.abh2169
- 42 Taki T, Akiyama M, Saito S, Ono R, Taniwaki M, Kato Y, Yuza Y, Eto Y, Hayashi Y: The *MYO1F*, unconventional myosin type 1F, gene is fused to *MLL* in infant acute monocytic leukemia with a complex translocation involving chromosomes 7, 11, 19 and 22. *Oncogene* 24(33): 5191-5197, 2005. DOI: 10.1038/sj.onc.1208711
- 43 Duhoux FP, Ameye G, Libouton J, Bahloulou K, Iossifidis S, Chantrain CF, Demoulin JB, Poirel HA: The t(11;19)(q23;p13) fusing *MLL* with *MYO1F* is recurrent in infant acute myeloid leukemias. *Leuk Res* 35(9): e171-e172, 2011. DOI: 10.1016/j.leukres.2011.04.022
- 44 Abate F, da Silva-Almeida AC, Zairis S, Robles-Valero J, Couronne L, Khiabani H, Quinn SA, Kim MY, Laginestra MA, Kim C, Fiore D, Bhagat G, Piris MA, Campo E, Lossos IS, Bernard OA, Inghirami G, Pileri S, Bustelo XR, Rabadan R, Ferrando AA, Palomero T: Activating mutations and translocations in the guanine exchange factor *VAV1* in peripheral T-cell lymphomas. *Proc Natl Acad Sci USA* 114(4): 764-769, 2017. DOI: 10.1073/pnas.1608839114
- 45 Cortes JR, Filip I, Albero R, Patiño-Galindo JA, Quinn SA, Lin WW, Laurent AP, Shih BB, Brown JA, Cooke AJ, Mackey A, Einson J, Zairis S, Rivas-Delgado A, Laginestra MA, Pileri S, Campo E, Bhagat G, Ferrando AA, Rabadan R, Palomero T: Oncogenic *Vav1-Myo1f* induces therapeutically targetable macrophage-rich tumor microenvironment in peripheral T cell lymphoma. *Cell Rep* 39(3): 110695, 2022. DOI: 10.1016/j.celrep.2022.110695
- 46 Morrish E, Wartewig T, Kratzert A, Rosenbaum M, Steiger K, Ruland J: The fusion oncogene *VAV1-MYO1F* triggers aberrant T-cell receptor signaling *in vivo* and drives peripheral T-cell lymphoma in mice. *Eur J Immunol* 53(3): e2250147, 2023. DOI: 10.1002/eji.202250147
- 47 McCormick JA, Ellison DH: The WNKs: atypical protein kinases with pleiotropic actions. *Physiol Rev* 91(1): 177-219, 2011. DOI: 10.1152/physrev.00017.2010
- 48 Tang BL: (WNK)ing at death: With-no-lysine (Wnk) kinases in neuropathies and neuronal survival. *Brain Res Bull* 125: 92-98, 2016. DOI: 10.1016/j.brainresbull.2016.04.017
- 49 Murillo-de-Ozores AR, Rodríguez-Gama A, Carbajal-Contreras H, Gamba G, Castañeda-Bueno M: WNK4 kinase: from structure to physiology. *Am J Physiol Renal Physiol* 320(3): F378-F403, 2021. DOI: 10.1152/ajprenal.00634.2020
- 50 Wilson FH, Disse-Nicodème S, Choate KA, Ishikawa K, Nelson-Williams C, Desitter I, Gunel M, Milford DV, Lipkin GW, Achard JM, Feely MP, Dussol B, Berland Y, Unwin RJ, Mayan H, Simon DB, Farfel Z, Jeunemaitre X, Lifton RP: Human hypertension caused by mutations in WNK kinases. *Science* 293(5532): 1107-1112, 2001. DOI: 10.1126/science.1062844
- 51 Golbang AP, Murthy M, Hamad A, Liu CH, Cope G, Van't Hoff W, Cuthbert A, O'Shaughnessy KM: A new kindred with pseudohypoaldosteronism type II and a novel mutation (564D>H) in the acidic motif of the *WNK4* gene. *Hypertension* 46(2): 295-300, 2005. DOI: 10.1161/01.HYP.0000174326.96918.d6
- 52 Boyden LM, Choi M, Choate KA, Nelson-Williams CJ, Farhi A, Toka HR, Tikhonova IR, Bjornson R, Mane SM, Colussi G, Lebel M, Gordon RD, Semmekrot BA, Poujol A, Välimäki MJ, De Ferrari ME, Sanjad SA, Gutkin M, Karet FE, Tucci JR, Stockigt JR, Kepler-Noreuil KM, Porter CC, Anand SK, Whiteford ML, Davis ID, Dewar SB, Bettinelli A, Fadrowski JJ, Belsha CW, Hunley TE, Nelson RD, Trachtman H, Cole TR, Pinsk M, Bockenhauer D, Shenoy M, Vaidyanathan P, Foreman JW, Rasoulpour M, Thameem F, Al-Shahrouri HZ, Radhakrishnan J, Gharavi AG, Goilav B, Lifton RP: Mutations in kelch-like 3 and cullin 3 cause hypertension and electrolyte abnormalities. *Nature* 482(7383): 98-102, 2012. DOI: 10.1038/nature10814
- 53 Carbajal-Contreras H, Gamba G, Castañeda-Bueno M: The serine-threonine protein phosphatases that regulate the thiazide-sensitive NaCl cotransporter. *Front Physiol* 14: 1100522, 2023. DOI: 10.3389/fphys.2023.1100522
- 54 Huang CL, Cheng CJ: A unifying mechanism for WNK kinase regulation of sodium-chloride cotransporter. *Pflugers Arch* 467(11): 2235-2241, 2015. DOI: 10.1007/s00424-015-1708-2
- 55 Argai ER, Gamba G: The regulation of Na⁺Cl⁻ cotransporter by with-no-lysine kinase 4. *Curr Opin Nephrol Hypertens* 25(5): 417-423, 2016. DOI: 10.1097/mnh.0000000000000247
- 56 Chen JC, Lin MX, Cheng CJ: WNK4 kinase: role of chloride sensing in the distal convoluted tubule. *Curr Opin Nephrol Hypertens* 30(2): 166-172, 2021. DOI: 10.1097/mnh.0000000000000683
- 57 Taylor CA 4th, Cobb MH: CCT and CCT-like modular protein interaction domains in WNK signaling. *Mol Pharmacol* 101(4): 201-212, 2022. DOI: 10.1124/molpharm.121.000307
- 58 Piovesan D, Del Conte A, Clementel D, Monzon AM, Bevilacqua M, Aspromonte MC, Iserte JA, Orti FE, Marino-Buslje C, Tosatto SCE: MobiDB: 10 years of intrinsically disordered proteins. *Nucleic Acids Res* 51(D1): D438-D444, 2023. DOI: 10.1093/nar/gkac1065
- 59 Babu MM: The contribution of intrinsically disordered regions to protein function, cellular complexity, and human disease.

- Biochem Soc Trans 44(5): 1185-1200, 2016. DOI: 10.1042/BST20160172
- 60 Bondos SE, Dunker AK, Uversky VN: On the roles of intrinsically disordered proteins and regions in cell communication and signaling. *Cell Commun Signal* 19(1): 88, 2021. DOI: 10.1186/s12964-021-00774-3
- 61 Bondos SE, Dunker AK, Uversky VN: Intrinsically disordered proteins play diverse roles in cell signaling. *Cell Commun Signal* 20(1): 20, 2022. DOI: 10.1186/s12964-022-00821-7
- 62 Malagrino F, Pennacchietti V, Santorelli D, Pagano L, Nardella C, Diop A, Toto A, Gianni S: On the effects of disordered tails, supertertiary structure and quinary interactions on the folding and function of protein domains. *Biomolecules* 12(2): 209, 2022. DOI: 10.3390/biom12020209
- 63 Gógl G, Kornev AP, Reményi A, Taylor SS: Disordered protein kinase regions in regulation of kinase domain cores. *Trends Biochem Sci* 44(4): 300-311, 2019. DOI: 10.1016/j.tibs.2018.12.002
- 64 Kato G: Regulatory roles of the N-terminal intrinsically disordered region of modular Src. *Int J Mol Sci* 23(4): 2241, 2022. DOI: 10.3390/ijms23042241
- 65 Pei J, Cong Q: Computational analysis of regulatory regions in human protein kinases. *Protein Sci* 32(10): e4764, 2023. DOI: 10.1002/pro.4764
- 66 Sharma S, Schiller MR: The carboxy-terminus, a key regulator of protein function. *Crit Rev Biochem Mol Biol* 54(2): 85-102, 2019. DOI: 10.1080/10409238.2019.1586828
- 67 Hurley JH: The ESCRT complexes. *Crit Rev Biochem Mol Biol* 45(6): 463-487, 2010. DOI: 10.3109/10409238.2010.502516
- 68 Hurley JH, Hanson PI: Membrane budding and scission by the ESCRT machinery: it's all in the neck. *Nat Rev Mol Cell Biol* 11(8): 556-566, 2010. DOI: 10.1038/nrm2937
- 69 Shilatifard A, Lane WS, Jackson KW, Conaway RC, Conaway JW: An RNA polymerase II elongation factor encoded by the human *ELL* gene. *Science* 271(5257): 1873-1876, 1996. DOI: 10.1126/science.271.5257.1873
- 70 Shilatifard A: Identification and purification of the Holo-ELL complex. *J Biol Chem* 273(18): 11212-11217, 1998. DOI: 10.1074/jbc.273.18.11212
- 71 Schmidt AE, Miller T, Schmidt SL, Shiekhattar R, Shilatifard A: Cloning and characterization of the EAP30 subunit of the ELL complex that confers derepression of transcription by RNA polymerase II. *J Biol Chem* 274(31): 21981-21985, 1999. DOI: 10.1074/jbc.274.31.21981
- 72 Kamura T, Burian D, Khalili H, Schmidt SL, Sato S, Liu WJ, Conrad MN, Conaway RC, Conaway JW, Shilatifard A: Cloning and characterization of ELL-associated proteins EAP45 and EAP20. *J Biol Chem* 276(19): 16528-16533, 2001. DOI: 10.1074/jbc.M010142200
- 73 Gross S, Rahal R, Stransky N, Lengauer C, Hoeflich KP: Targeting cancer with kinase inhibitors. *J Clin Invest* 125(5): 1780-1789, 2015. DOI: 10.1172/JCI76094
- 74 Cicenas J, Zalyte E, Bairoch A, Gaudet P: Kinases and cancer. *Cancers (Basel)* 10(3): 63, 2018. DOI: 10.3390/cancers10030063
- 75 Roskoski R Jr: Targeting oncogenic Raf protein-serine/threonine kinases in human cancers. *Pharmacol Res* 135: 239-258, 2018. DOI: 10.1016/j.phrs.2018.08.013
- 76 Roskoski R Jr: Targeting ERK1/2 protein-serine/threonine kinases in human cancers. *Pharmacol Res* 142: 151-168, 2019. DOI: 10.1016/j.phrs.2019.01.039
- 77 Turdo A, D'Accardo C, Glaviano A, Porcelli G, Colarossi C, Colarossi L, Mare M, Faldetta N, Modica C, Pistone G, Bongiorno MR, Todaro M, Stassi G: Targeting phosphatases and kinases: How to checkmate cancer. *Front Cell Dev Biol* 9: 690306, 2021. DOI: 10.3389/fcell.2021.690306
- 78 Lee PY, Yeoh Y, Low TY: A recent update on small-molecule kinase inhibitors for targeted cancer therapy and their therapeutic insights from mass spectrometry-based proteomic analysis. *FEBS J* 290(11): 2845-2864, 2023. DOI: 10.1111/febs.16442
- 79 Roskoski R Jr: Properties of FDA-approved small molecule protein kinase inhibitors: A 2023 update. *Pharmacol Res* 187: 106552, 2023. DOI: 10.1016/j.phrs.2022.106552

Received February 8, 2024

Revised March 17, 2024

Accepted March 20, 2024